

## MIT Open Access Articles

*Cancer Cell–Derived Matrisome Proteins Promote Metastasis in Pancreatic Ductal Adenocarcinoma*

The MIT Faculty has made this article openly available. **Please share** how this access benefits you. Your story matters.

**Citation:** Tian, Chenxi et al. "Cancer Cell–Derived Matrisome Proteins Promote Metastasis in Pancreatic Ductal Adenocarcinoma." *Cancer Research* 80, 7 (February 2020): dx.doi.org/10.1158/0008-5472.can-19-2578 © 2020 American Association for Cancer Research

**As Published:** <http://dx.doi.org/10.1158/0008-5472.can-19-2578>

**Publisher:** American Association for Cancer Research (AACR)

**Persistent URL:** <https://hdl.handle.net/1721.1/128828>

**Version:** Author's final manuscript: final author's manuscript post peer review, without publisher's formatting or copy editing

**Terms of use:** Creative Commons Attribution-Noncommercial-Share Alike





Published in final edited form as:

*Cancer Res.* 2020 April 01; 80(7): 1461–1474. doi:10.1158/0008-5472.CAN-19-2578.

## Cancer-cell-derived matrisome proteins promote metastasis in pancreatic ductal adenocarcinoma

Chenxi Tian<sup>1</sup>, Daniel Öhlund<sup>2,3,4</sup>, Steffen Rickelt<sup>1</sup>, Tommy Lidström<sup>3,4</sup>, Ying Huang<sup>1</sup>, Liangliang Hao<sup>1</sup>, Renee T. Zhao<sup>1</sup>, Oskar Franklin<sup>5</sup>, Sangeeta N. Bhatia<sup>1,6</sup>, David A. Tuveson<sup>2</sup>, Richard O. Hynes<sup>1,6,\*</sup>

<sup>1</sup>Koch Institute for Integrative Cancer Research, Massachusetts Institute of Technology, Cambridge, MA 02139

<sup>2</sup>Cold Spring Harbor Laboratory, Cold Spring Harbor, NY 11724

<sup>3</sup>Department of Radiation Sciences, Umeå University, Umeå, Sweden

<sup>4</sup>Wallenberg Centre for Molecular Medicine, Umeå University, Umeå, Sweden

<sup>5</sup>Department of Surgical and Perioperative Sciences, Umeå University

<sup>6</sup>Howard Hughes Medical Institute

### Abstract

The prognosis for pancreatic ductal adenocarcinoma (PDAC) remains poor despite decades of effort. The abundant extracellular matrix (ECM) in PDAC comprises a major fraction of the tumor mass and plays various roles in promoting resistance to therapies. However, non-selective depletion of ECM has led to poor patient outcomes. Consistent with that observation, we previously showed that individual matrisome proteins derived from stromal cells correlate with either long or short patient survival. In marked contrast, those derived from cancer cells correlate strongly with poor survival. Here we studied three cancer-cell-derived matrisome proteins that are significantly overrepresented during PDAC progression; AGRN (agrin), SERPINB5 (serine protease inhibitor B5), and CSTB (cystatin B). Using both overexpression and knockdown experiments, we demonstrate that all three are promoters of PDAC metastasis. Furthermore, these proteins operate at different metastatic steps. AGRN promoted EMT in primary tumors, whereas SERPINB5 and CSTB enhanced late steps in the metastatic cascade by elevating invadopodia formation and *in vivo* extravasation. All three genes were associated with a poor prognosis in human patients and high levels of SERPINB5, secreted by cancer cells and deposited in the ECM, correlated with poor patient prognosis. This study provides strong evidence that cancer-cell-derived matrisome proteins can be causal in promoting tumorigenesis and metastasis and lead to poor patient survival. Therefore, compared with the bulk matrix, mostly made by stromal cells, precise interventions targeting cancer-cell-derived matrisome proteins, such as AGRN, SERPINB5, and CSTB, may represent preferred potential therapeutic targets.

\*Corresponding author. rohynes@mit.edu. Koch Institute for Integrative Cancer Research, Room 76-361D, Massachusetts Institute of Technology, Cambridge, MA 02139 USA, TEL: 617-253-6422.

The authors declare no potential conflicts of interest.

## INTRODUCTION

Prognosis for pancreatic ductal adenocarcinoma (PDAC) remains dismal, with 5-year survival rate being less than 9% (1). PDAC is characterized by a pronounced resistance to radiation, cytotoxic agents, and targeted and immuno-therapies (2). PDAC has highly desmoplastic stroma, constituting a major fraction (up to 90%) of the tumor mass and composed of a variety of non-neoplastic cell types and extracellular matrix (ECM). The chemo- and radiotherapeutic resistance of PDAC is thought to be mediated, at least in part, by its prominent ECM, which compresses blood vessels resulting in inefficient drug delivery and promoting survival through integrin-mediated signaling pathways (3). However, non-selective depletion of stroma by targeting the ECM-inducing Hedgehog signaling pathway (4) or depleting  $\alpha$ -smooth-muscle-actin-positive fibroblast cells (5) in mice resulted in poorly differentiated cancer cells and poor survival, despite successful depletion of stroma and enhanced drug uptake. Similarly, clinical trials targeting metastatic PDAC using Smoothed inhibitor blockade of Hedgehog signaling were halted because of paradoxical acceleration of disease progression (6). Thus, the prominent ECM in PDAC appears to have a dual nature, at times even restraining pancreatic cancer progression.

During cancer progression, ECM deposited by both cancer cells and various stromal cells (7,8), plays both biophysical and biochemical roles to regulate malignant cell behaviors. For example, in the tumor microenvironment, ECM proteins can directly promote oncogenic transformation and metastasis, and influence stromal cell behaviors, such as angiogenesis and inflammation, resulting in formation of a pro-tumorigenic microenvironment (9). In distant organs, ECM proteins have been shown to contribute to metastatic niches that maintain cancer cell stemness and enable cancer cell outgrowth (10,11). The matrisome is defined as both core ECM proteins, including collagens, glycoproteins and proteoglycans, and ECM-associated proteins, such as ECM regulators (e.g., proteases and their inhibitors, cross-linking agents), ECM-affiliated proteins (e.g., mucins, lectins, annexins), and secreted factors (e.g., growth factors, chemokines) (8). We and others have used liquid chromatography-tandem mass spectrometry (LC-MS/MS) to define the matrisome compositions in mouse tumorigenic models, as well as human tumors (12), and such studies have revealed previously unknown, functionally relevant promoters of cancer progression.

In a recent study we applied quantitative MS-based proteomic approaches to systematically profile the composition and dynamics of ECM proteins during PDAC progression in both mouse genetic PDAC models and human patient samples (13). We identified over 200 matrisome proteins that are significantly overrepresented in PDAC compared to normal pancreas in human samples and assigned cancer-cell vs. stromal origin to a majority of them. We found that high levels of ECM proteins derived from tumor cells, rather than those exclusively produced by stromal cells, tend to correlate with poor patient survival, while stromal-cell-derived ECM proteins can either positively or negatively correlate with survival. That study supported the hypothesis that PDAC stroma has a dual role and argued [1] against non-selective depletion of stroma, and [2] that cancer-cell-derived matrisome proteins may be potential therapeutic targets.

In this study, we selected three cancer-cell-derived matrisome proteins that are overrepresented in PDAC; AGRN, SERPINB5, and CSTB, and performed functional studies *in vivo*. These experiments revealed their functions in promoting different steps of metastasis. We also showed that high expression levels of all three genes correlate with poor patient survival. These results demonstrate that the detailed proteomic analysis of PDAC tumor ECM can identify clinically relevant ECM proteins promoting tumor development and metastasis, which are potential candidates for future focused therapeutic interventions.

## MATERIALS AND METHODS

### Cell line maintenance and mouse strains

The MIT Animal Care and Use Committees reviewed and approved all animal studies and procedures. NOD/SCID/IL2R $\gamma$ -null mice were used throughout the study (Jackson Laboratory, Bar Harbor, ME). The human pancreatic adenocarcinoma cell lines AsPC1 and BxPC3 were purchased from American Type Cell Culture (ATCC, Manassas, VA), where they were tested and authenticated. The human CAF cell line hT1 was published previously (14). AsPC1 was cultured in RPMI medium 1640 (Thermo Scientific, Pittsburgh, PA) and the other cell lines were cultured in HyClone high-glucose Dulbecco's modified Eagle's medium (Thermo Scientific, Pittsburgh, PA), supplemented with 10% fetal bovine serum (Invitrogen, Carlsbad, CA) at 37°C in a 5% CO<sub>2</sub> incubator.

### Generation of *in vivo* selected BxPC3 cell lines

BxPC3 G1.1 cells were *in vivo*-selected from parental BxPC3 cells through three rounds of metastasis in 8–10-week-old NOD/SCID/IL2R $\gamma$ -null mice (Jackson Laboratory, Bar Harbor, ME) For each round of selection,  $1 \times 10^6$  cells in 50ul PBS were implanted into the pancreas, 4 weeks later lung metastatic nodules were removed aseptically and treated with type I collagenase (17018029, ThermoFisher) following the product manual and cells were grown *in vitro*. The resulting cells were implanted in the pancreas for the next round of selection. For ease of quantification all the cells were rendered ZsGreen-positive by retroviral infection with MSCV-puromycin-IRES-ZsGreen.

### CRISPR activation

AsPC1 cells stably expressing dCas9-VP64-Blast (Addgene #61425) and MS2-P65-Hygro (Addgene #61426) were generated through sequential lentiviral transduction and selection with Blasticidin and Hygromycin, respectively (15). The resulting AsPC1 cells were then transduced with lentiviral vector (Lenti-sgRNA-MS2-Zeocin; Addgene #61427) inserted with gRNA targeting promoter sequences of each gene and subsequently zeocin-selected to generate the final cell lines stably overexpressing genes of interest. The target gRNA sequences were designed using the SAM website (<http://sam.genome-engineering.org>). We tested 5 to 10 different gRNAs and selected two gRNAs that led to the best overexpression of the genes of interest. The gRNAs selected were as follows, with PAM sequences in bold:

*CSTB* 1 TTTCCGGGCGCCGAGTCACAC**GG**;

*CSTB* 2 CGGAAAGACGATACCAGCCCC**GG**;

*AGRN1* AGGGGGAGGAGGAGGGCGCGGGG;

*AGRN2* GACAGGACGGGACGCAGCTCCGG;

*SERPINB51* AGCTGCCAAGAGGCTTGAGTAGG;

*SERPINB52* ATTGTGGACAAGCTGCCAAGAGG.

### CRISPR inactivation

BxPC3 G1.1 cells were transduced with pHR-TRE3G-KRAB-dCas9-P2A-Blast lentivirus, which is modified from a construct (Addgene #60954) by replacing SFFV promoter with a doxycyclin-inducible promoter TRE3G and mCherry with Blasticidin sequence, and selected with Blasticidin (16). The cells were then transduced with pHR-SFFV-TET3G at 1:10 dilution without selection (kind gift from Luke Gilbert in the Weissman lab, UCSF). The resulting cells were then transduced with lentiviral vector that is modified lentiGuide-Puro (lentiGuide-Puro, Addgene #52963) by replacing puro with tdTomato sequence and sorted by fluorescence-activated cell sorting for cells positive for tdTomato. The gRNA sequences were targeted against -50 to 200bp of the transcription start site of each gene (16). We tested 5 to 15 different gRNAs in the presence of doxycycline and selected gRNAs that knocked down the genes of interest to the greatest extent. The gRNAs selected are as follows, with PAM sequences in bold:

*CSTB1* CGCCGCCAAGATGATGTGCGGGG;

*SERPINB51* AGCTGCCAAGAGGCTTGAGTAGG;

*SERPINB52* ACACGGTCGCCTCCACATCCAGG

*AGRN1* GGTGCTCACCGGGACGGTGGAGG;

*AGRN2* GTCCAGTCCCGTCCCCGGCGCGG.

Both control and experimental mice were fed with DOX diet (Bio-serv) throughout the experiment.

### Orthotopic and tail-vein implantation

For CRISPR-SAM-activation and CRISPR-inactivation experiments,  $1 \times 10^5$  cells in 50ul PBS were injected into pancreata of 8–10-week-old NOD/SCID/IL2R $\gamma$ -null (NSG) mice (Jackson Laboratory, Bar Harbor, ME). Tumors were harvested 6 (CRISPR-inactivation) or 10 (CRISPR-SAM-activation) weeks post-injection. For tail-vein injection,  $5 \times 10^4$  cells in 100ul PBS were injected into the lateral tail vein of 8- to 12-week-old NSG mice. The mice were sacrificed 6 weeks later and lungs were imaged by fluorescence microscopy and then fixed overnight with 4% paraformaldehyde solution in PBS (Santa Cruz). Samples were kept in 70% ethanol prior to embedding and sectioning. All procedures were performed according to an animal protocol approved by MIT's Department of Comparative Medicine and Committee on Animal Care.

### Quantification of metastases

ZsGreen-positive metastatic load was quantified using imageJ in the left pulmonary lobe. Metastasis load in the left lobe is representative of all lung lobes. Thresholding method was chosen for each experiment. Manual curation was applied when necessary. Two-tailed Student's t test was performed to evaluate the statistical significance of the results.

### Extravasation assay

Cells ( $2 \times 10^5$  in 100 $\mu$ l PBS) were injected via lateral tail vein into NSG mice. 24 hours after injection mice were euthanized and lungs were collected after inflation with 4% paraformaldehyde solution and 0.3% Triton X-100. Fixed lungs were cut into 0.5mm slices and stained with anti-CD31 (5533070, BD Biosciences) and Alexa 594-conjugated goat anti-rat IgG (Molecular Probes). Scoring was done blindly. Images were taken with a Nikon A1R laser-scanning confocal microscope using a 40x objective and tumor cells were scored as intravascular or extravascular.

### Immunohistochemistry

Tissues (lungs and pancreas) were fixed in 4% paraformaldehyde solution or 10% neutral-buffered formalin at room temperature overnight and paraffin-embedded following standard procedures. Consecutive sections were prepared using a Leica RM2255 rotary microtome (Leica Biosystems, Nussloch, Germany) and dried at 60°C for 1h. The sections were then dewaxed and rehydrated before staining with hematoxylin and eosin (H&E) or treatment with heat-induced epitope-retrieval (HIER) using a decloaking chamber (Biocare medical, Concord, CA) prior to immunostaining. The sections were incubated in 10 mM sodium citrate (pH6.0) or 10mM Tris (pH9.0) buffered solutions containing 0.05% Tween at 120°C for 2min using a pressure cooker (HIER step). If needed, additional enzyme treatment using pepsin was included. To obtain consistent and reliable staining on all tissues investigated, an automated staining system (LabVision Autostainer 360, Thermo Scientific, Fremont, CA) was used. To destroy all endogenous peroxidase and alkaline phosphatase activity in the tissue, the sections were subsequently pretreated using BLOXALL endogenous enzyme blocking solution (Vector Laboratories, Burlingame, CA, USA) for 10 min. After a blocking step with normal serum, the sections were incubated with the individual primary antibodies for 1h followed by secondary ImmPRESS polymer detection systems (Vector Laboratories, Burlingame, CA) according to the manufacturer's protocol. The Vulcan Fast Red Chromogen Kit 2 (red staining; Biocare Medical, Concord, CA, USA) and the DAB Quanto Substrate System (brown staining; Thermo Scientific, Fremont, CA) were applied as substrates. For multi-color IHC stainings, following HIER and blocking steps, the individual antibodies were incubated consecutively using the chromogens indicated above. For counterstaining, hematoxylin was used. Primary antibodies used were: AGRN (Novus Biologicals, Littleton, CO, NBP1-90209), CDH1 (BD Biosciences, San Jose, CA, 610181), CSTB (Abcam, Cambridge, MA, ab53725), LMNA (human specific; Abcam, ab108595), SERPINB5 (Origene, Rockville, MD, TA-322980), VIM (human specific; Leica Biosystems, Nussloch, Germany, NCL-L-VIM-V9), ZEB1 (Sigma-Aldrich, St. Louis, MO, HPA027524).

### Immunoblotting of tumor samples, cells and cell culture media

Tumor samples were lysed in Laemmli buffer, proteins were separated by SDS-PAGE (4–20% gradient gel from Biorad) and immunoblotting was performed using the following antibodies: GAPDH (Millipore, Bedford, MA, MAB374), AGRN (Novus Biologicals, Littleton, CO, NBP1–90209), SERPINB5 (Origene, Rockville, MD, TA-322980), CSTB (Abcam, Cambridge, MA, ab53725). Chemiluminescence development was done using Tanon 5200CE. To collect cell culture media for immunoblotting, freshly confluent control BxPC3 cells and those overexpressing SERPINB5 or CSTB by CRISPR-SAM method are cultured in CHO media (Hyclone) for 2 days. The supernatant was high-speed centrifuged to remove cell debris and concentrated 10-fold by Amicon centrifugal filters (EMD Millipore).

### Reverse transcription and quantitative real-time PCR

RNA was isolated from cell or tumor lysates using an RNeasy kit (Qiagen, Germantown, MD) and cDNA was synthesized by reverse transcription using the First-Strand cDNA Synthesis Kit (Promega, Madison, WI). qPCR reactions were performed using Bio-Rad SYBR Green Supermix (Bio-Rad, Hercules, CA) according to the manufacturer's instructions. qPCR results were analyzed in Excel. Student's t test was performed to evaluate the statistical significance of differences between groups. Human and murine PCR primers used are listed in Table S1.

### RNA in situ hybridization

Formalin-fixed paraffin-embedded tissue was sectioned (4 $\mu$ m) and analyzed for SERPINB5 and Cytokeratin-19 (*KRT19*) expression using ViewRNA™ ISH Tissue Assay Kit (ThermoFisher), with probes against *SERPINB5* (VA1–12247-VT) and cytokeratin-19 (VA6–10947-VT) (ThermoFisher), according to manufacturer's protocol. In short: tissue was deparaffinized in Xylene and 100% ethanol. The sections were pretreated for 10min at 90–95°C, followed by protease digestion for 10min at 40°C and then fixed in 10% normal buffered formalin followed by hybridization with the target probes against SERPINB5 and KRT19 for 2h in 40°C. The sections were stored overnight in storage buffer before proceeding with signal amplification and detection. The sections were preamplified for 25min at 40°C followed by amplifier hybridization for 15min at 40°C. Followed by incubation with label probes at 40°C for 15min and addition of substrate. FastRed label probe and substrate incubation was performed first. Sections were then counterstained in Gil's hematoxylin, dipped in 0.01% ammonium hydroxide followed by DAPI staining (1 $\mu$ g/ml for 10min). Slides were mounted with Prolong gold antifade mountant with DAPI (ThermoFisher). The confocal images were taken on a Zeiss LSM 710 microscope and the IHC images were scanned on the 3DHISTECH Panoramic 250 flash III.

### Quantification of double-color IHC images

Double-color IHC images were taken at 20x (ZEB1) and 10x (VIM and CDH1) to cover all the regions in each tumor. A macro was written to perform image quantification in imageJ. Specifically, color deconvolution was used to separate the red and brown channels, and then the two channels were thresholded and outlined with the “Yen” algorithm. Then for each nucleus that is positive for LMNA, the program decides if the cell is also positive in the



second channel. Finally, the positive cell fraction is calculated. For each tumor, at least 2000 cells covering the entire tumor region were quantified. Two-tailed Student's t test was performed to evaluate the statistical significance of the results.

### **Tissue samples and tissue microarray construction**

The tissue microarray (TMA) was constructed from cancer specimens of patients that underwent surgery for PDAC between 1990–2009 at Umeå University Hospital. All participating individuals provided written informed consent. The study was conducted in accord with the Helsinki Declaration of 1975 and was approved by the regional research ethics board of northern Sweden (Dnr. 09–175M/2009–1378-31). Core areas of 1 mm in diameter were first selected by an experienced pathologist, then drilled and placed on recipient blocks using a TMA Grand master machine (3DHISTECH, Budapest, Hungary). Three cores were included from each primary tumor (n=75) and 1–3 cores from metastatic lymph nodes (n=32). The cores were coded and randomly placed on the recipient blocks. Clinical data were retrieved from hospital charts. Scoring of at least two tissue cores per patient was required for comparison of staining intensity to survival. The observers were blinded for the clinical information during analysis of tissue staining. Normal pancreatic tissue was collected as control from patients undergoing pancreatic surgery for non-malignant conditions (n=4).

### **IHC Scoring for human TMA**

IHC staining intensity was analyzed by two independent investigators. Stromal and epithelial intensity were semi-quantitatively scored (1=low intensity, 2=moderate intensity, 3=high intensity, 4=Very high intensity). When Scoring differed between investigators the mean of the differing scores was used. Patients were divided into high (intensity score>2) and low intensity (intensity score<=2) groups, and their survival was compared. Mantel-Cox test was used to calculate P values.

### **Gelatin degradation assay and immunofluorescence staining**

To label cover slips with fluorescent gelatin, 18 mm circular No. 2 cover glasses (VWR) were washed with a 2:1 mixture of nitric to hydrochloric acid for 2 hr, rinsed with 70% ethanol, then coated with 50 µg/ml poly-D-lysine for 20 min and fixed with 0.5% glutaraldehyde for 15 min. After washing with PBS, cover slips were then coated with Alexa Fluor 594-gelatin (ThermoFisher, A20004) mixed with 2% sucrose. Alexa Fluor 594-gelatin was generated following a protocol described elsewhere (17). Cover slips were then coated with 20 µg/ml fibronectin (Advanced BioMatrix) and quenched with 5 mg/ml sodium borohydride (Sigma). 30,000 cells were added to each gelatin-coated cover slip. AsPC1 cells were fixed 20 hours after plating with 4% paraformaldehyde and stained with .5 µg/ml DAPI (ThermoFisher). TKS5 immunofluorescence staining followed a published protocol (18). In short, AsPC1 cells were plated on gelatin-coated coverslips that were prepared using the same method as for the gelatin degradation assay for 20 hours. Then the cells were fixed with 4% paraformaldehyde, blocked, and incubated first with 2 mg/ml of TKS5 antibody (clone 13H6.3, MilliporeSigma, MABT336) and then with Alexa Fluor-488 or -594 anti-mouse IgG (ThermoFisher). All images for gelatin degradation assay and TKS5+ invadopodia quantification assay were taken with a Nikon A1R laser-scanning confocal



microscope using a 40x objective and then quantified with ImageJ. For each cell line, at least 20 fields were counted with at least 16 cells per field.

### **Proliferation assay**

The assays were performed in the Incucyte Zoom System (Essen Bioscience). For proliferation, 10,000 cells were seeded in triplicate into 96-well plate to reach 10% confluence. Phase-contrast images were captured every 3 hours to calculate percent confluency. At least 10 fields were quantified for each cell line. P values were individually calculated by Student's t test for the last 12 hours (last four time points), and then were corrected for multiple testing using the Benjamini-Hochberg method. The highest adjusted p value among the four points for each cell line were represented by star(s). \*,  $p < 0.05$ ; \*\*,  $p < 0.01$ ; \*\*\*,  $p < 0.001$ ; \*\*\*\*,  $p < 0.0001$ . ns, not significant.

### **Survival analysis**

Gene expression and clinical data for human pancreatic ductal adenocarcinoma (TCGA) were downloaded from cBioportal (19). Gene expression data were Z-score normalized. For each gene, we calculated the log-rank p values and hazard ratios by determining the overall survival differences in categorized patients using quartile expression values (top vs. bottom quartile). The Cox regression analyses were done using the R package OISurv.

### **Recombinant protease and cell lysate substrate cleavage assay**

Protease substrates with fluorescence (FAM) and quencher (CPQ2) were synthesized by CPC Scientific Inc. Peptide sequences are as following: Q3, PVGLIG; Q6, PLGLRSW; PQ19, PVPLSLVM; PQ2, GGSGRSANAK. In recombinant protease cleavage assay, protease vendor and buffer conditions were: MMPs (Enzo) (50mM TRIS, pH 7.5, 10 mM CaCl<sub>2</sub>, 300 mM NaCl, 20 μM ZnCl<sub>2</sub>, 0.02% Brij-35, 1% BSA); ADAMs (Enzo) (10 mM HEPES, pH 7.4, 100 mM NaCl, 0.01% Brij-35, 1% BSA); uPA (R&D) (50 mM Tris, 0.01% Tween 20, pH 7.4, 1% BSA); Cathepsin B (R&D) (25 mM MES, 5 mM DTT, pH 5.0); Cathepsin D (R&D) (0.1 M NaOAc, 0.2 M NaCl, pH 3.5); Cathepsin E (R&D) (0.1 M NaOAc, 0.5 M NaCl, pH 3.5); Cathepsin K (Enzo) (50mM NaOAc, 1mM DTT, pH 5.5); Cathepsin L (R&D) (50 mM MES, 5 mM DTT, 1 mM EDTA, 0.005% (w/v) Brij-35, pH 6.0). In the cell lysates cleavage assay, cell lysates were freshly prepared in lysis buffer (1% NP-40, 0.15M NaCl, 10mM Tris, pH7.5) with and without 1mM EDTA at 2 mg/mL prior to assay. Assays were performed in the 384-well plate in triplicate in enzyme-specific buffer with peptides (1 μM) and proteases (40 nM) in 30 μL at 37 °C. Fluorescence was measured at Ex/Em 495/535nm using a Tecan Infinite 200pro microplate reader (Tecan). Signal increase at 60 minutes was monitored at 2mins interval across conditions. Initial cleavage rate was calculated using imageJ. Two-tailed t test was performed to compare the cell lysates to the control cell lines. Independent validation on the four peptide substrates was also published elsewhere (T3 is Q3, T6 is Q6, T56 is PQ19) (20).

## RESULTS

### AGRN, SERPINB5 and CSTB are upregulated in PDAC and correlate with poor patient survival

We previously used proteomics to identify matrisome proteins overrepresented during PDAC progression and found that high expression of many cancer-cell-derived matrisome proteins correlates with poor survival (published results summarized and illustrated in Figure 1A) (13). We wished to test directly whether ECM proteins differing between normal pancreas and PDAC might play causal roles during PDAC tumor progression. We selected three cancer-cell-derived proteins (AGRN, agrin; SERPINB5, serine protease inhibitor Family Member B5 or Maspin; CSTB, cysteine protease inhibitor B or cystatin B) based on the following criteria: (1) significantly overrepresented and abundantly present in human PDAC MS analyses (Figure 1B–D, Table S2); (2) expressed exclusively or mostly by the cancer cells (Figure 1A); (3) correlated with poor patient overall survival when highly expressed (Figure 1E–G); and (4) have not previously been functionally studied in PDAC progression and metastasis by *in vivo* experiments (Table S2). We confirmed that their RNA expression levels are increased during PDAC progression in the KPC mouse model (Figure 1H–J). By immunohistochemistry (IHC) we also confirmed that the expression levels of all three proteins are higher in PDAC compared with normal pancreas in both human and mouse samples/tissues (Figure 1K–M). AGRN is a heparan sulfate basal-lamina glycoprotein, and we observed it expressed predominantly in the basement membrane surrounding the diseased epithelial compartment (Figure 1K). SERPINB5 and CSTB, on the other hand, are more diffusely localized, both intracellularly and extracellularly (Figure 1L, M). Besides AGRN, SERPINB5 and CSTB, there are a few other proteins that also fit our selection criteria, including MXRA5, LMAN1 and S100A16, which could be interesting proteins for future studies (Table S2).

### Knockdown of AGRN, SERPINB, and CSTB in tumor cells reduces tumor growth and *in vivo* metastasis

To investigate their functions, we first used a CRISPR-driven inactivation system (16) to suppress expression of each of the three genes. The inactivation was performed in an *in-vivo*-selected highly lung-metastatic BxPC3 cell line, whose parental BxPC3 line has high expression levels for all three genes, based on data from the Cancer Cell Line Encyclopedia (CCLE, Figure S1A–C). For each gene, we screened a number of gRNA guides to select one or two gRNAs that most effectively knocked down expression at both mRNA and protein level (Figure 2A). We found that cells knocked down for each of the three genes grew more slowly in *in vitro* proliferation assays (Figure S2A).

In order to test the *in vivo* function of the three genes in primary tumor growth and metastasis, we orthotopically injected the control or knock-down cell lines for each gene into immunocompromised NOD/SCID/IL2R $\gamma$ -null (NSG) mice. We found that knocking down each of the three genes significantly reduced the primary tumor weight in the case of all gRNA guides tested (Figure 2B). We then monitored distant metastasis in both lungs and livers. We quantified metastasis by the percentage of ZsGreen-positive area in the left pulmonary lobe (Figure 2C, D) and also indicated metastasis by IHC with a human-specific

anti-LMNA antibody, since the cancer cells are of human origin (Figure 2E, F). We found that knocking down expression of each of the three genes led to significant decreases in the metastasis load normalized to the primary tumor weight with all gRNA guides tested in both lungs (Figure 2C, E) and liver (Figure 2D, F). Note that the lung-selected BxPC3 cell line is highly lung-metastatic and poorly liver-metastatic (comparing the y axes in Figure 2C and 2D). The liver metastases may not all result from hematogenous/lymphatic dissemination, because there may be direct cell transfer to the liver either from primary sites, or from ascites resulting from pancreatic tumors. This set of experiments established direct roles for AGRN, SERPINB5 and CSTB in promoting PDAC growth and metastasis.

### Overexpression of AGRN, SERPINB5, and CSTB in tumor cells increases metastasis

To investigate the functional roles of the three genes in a complementary experiment, we used the synergistic activation mediator (SAM) CRISPR/dCas9 gene activation system to induce expression of each of the three genes (15). The activation was performed in the AsPC1 cell line, which expresses lower levels of all three genes as compared with the BxPC3 cell line in CCLE (Figure S1). For each gene, we selected two gRNA guides that most effectively induced expression at both the mRNA and protein level (Figure 3A). Overexpressing the AGRN and SERPINB5 by both gRNAs and CSTB by one gRNA resulted in significant increases in *in vitro* proliferation for all gRNAs tested, although compared to the knockdown set of cells, the changes in proliferation were small (Figure S2B). Furthermore, we found that orthotopic tumor weights from these modified cells were not different from control cells (Figure 3B). The discordance between the *in vitro* proliferation assay and the *in vivo* tumor growth assay could be due to the differences between *in vitro* and *in vivo* environments, such as the interplay between cancer cells and various types of stromal cells. It is also possible that overexpressing the three genes is not sufficient alone to alter primary tumor growth, or that the effects are cell line specific. We then examined lung metastasis by normalizing the fraction of ZsGreen-positive area to primary tumor weight (Figure 3C, D). We discovered that overexpressing AGRN or SERPINB5 significantly increased lung metastasis using both guides tested for each (Figure 3C). CSTB overexpression led to significantly increased metastasis with one guide, and not significantly increased metastasis with the second guide, however, the p value (0.0529) is very close to being significant (Figure 3C). We could not quantify metastasis to the liver because liver metastasis was not evident from AsPC1 cells.

Combining the results from both knockdown and overexpression experiments, we conclude that [1] each of AGRN, SERPINB5 and CSTB is required for promotion of metastasis and can enhance metastasis to varying degrees; [2] they may play a small role in primary tumor growth.

### AGRN promotes epithelial-to-mesenchymal transition

Epithelial-to-mesenchymal transition (EMT) is known to regulate malignant cell motility, invasiveness and dissemination to form distant metastases (21). We asked whether the cancer-cell-derived proteins, AGRN, SERPINB5, and CSTB, could regulate EMT. We first confirmed by IHC that the xenograft tumors knocked down or overexpressing each of the three genes have the expected downregulation and upregulation of the corresponding

proteins (Figure S3A, B). We then confirmed these changes at the RNA level using qPCR primers that amplified the cDNA only from human cells but not from mouse tumors (Figure S3C, D, E).

To examine EMT, we performed double-color IHC in xenograft primary tumors knocked down or overexpressing each of the genes. Specifically, we used a human-specific anti-LMNA antibody to highlight cancer cells and quantified the percentage of LMNA+ cancer cells also positive for the mesenchymal markers, ZEB1, VIM, and the epithelial marker CDH1. AGRN knocked-down (kd) tumors have reduced proportions of ZEB1+, VIM+ and increased proportions of CDH1+ cancer cells (Figure 4A–C), while AGRN overexpression (oe) tumors had the opposite phenotypes (Figure 4D–F). However, knocking down and overexpressing SERPINB5 and CSTB did not have any impact on these EMT markers (Figure 4A–F). We also tested the expression of additional EMT markers by species-specific qPCR. We designed human (cancer cell) sequence-specific qPCR primers to amplify additional mesenchymal markers, TWIST1, SNAI1 and FN1, in the xenograft tumor cDNA (Figure S4A). AGRN kd, but not knockdowns of SERPINB5 or CSTB, reduced expression of these markers (Figure S4B). AGRN oe did not appear to change expression of TWIST1 and SNAI1 by qPCR statistically significantly. Consistent with that result, AGRN oe also had less impact on ZEB-1, VIM, and CDH1 as compared with AGRN kd in the double-color IHC experiment.

Collectively these results suggest that AGRN acts to promote EMT in primary tumors. This further implies that AGRN likely promotes metastasis partly through increasing the EMT program, which potentially regulates early metastasis steps, such as dissemination.

### **SERPINB5 and CSTB promote extravasation**

To test whether each of the three ECM proteins influenced later steps of the metastatic cascade (survival in the circulation, extravasation, and colonization), we tested the experimental pulmonary metastasis model. Specifically, we injected cancer cells, overexpressing or knocked down for each of the three genes, directly into the circulation via the lateral tail vein. We found that knocking down each of the three genes significantly reduced lung metastasis compared to controls (Figure 5A, S5A), and overexpression of all three genes significantly increased lung metastasis (Figure 5B, S5B). This suggests that all three genes can promote later steps of metastasis.

One key step in the late metastatic cascade is extravasation. Therefore, we performed an *in vivo* extravasation assay to test whether AGRN, SERPINB5 or CSTB promote extravasation. Specifically, we inoculated the overexpression set of cells into the lateral tail vein and counted the percentage of cells that were extravascular in the lungs using confocal microscopy. We chose 24h after injection over later time points to minimize the effect of cell division. We discovered that AGRN oe cells were comparable to the control cells in extravasation ratio, however, both SERPINB5 and CSTB oe cells showed significantly enhanced extravasation (Figure 5C, D). We could not perform extravasation assays on the kd set of BxPC3 cells because we observed that BxPC3 cells clustered together in the vasculature, making it impossible to quantify extravasation in single cells (Figure S5C). This

is possibly due to the fact that BxPC3 cells are bigger than AsPC1 cells and therefore they do not spread well in the lung vasculature.

Invadopodia are protrusive structures expressing MMP14 (MT1-MMP), which cleaves ECM and contributes to breaching the basement membrane, and they are required for cancer cell extravasation (22,23). We therefore tested invadopodial activity and quantified invadopodia-positive fraction in these cancer cells. Gelatin degradation assay is commonly used to test invadopodial activity. We quantified the fraction of cells that degraded gelatin, making dark spots on coverslips coated with Alexa Fluor 594-labeled gelatin, at 20 hours post-plating (Figure 5E). We discovered that cancer cells that overexpress SERPINB5 and CSTB were significantly better at degrading gelatin (Figure 5F) compared to AGRN or control cells. The degradation spots colocalized with TKS5-positive invadopodia in AsPC1 cells (Figure 5G, Figure S5D). Consistent with this correspondence, cancer cells that overexpress SERPINB5 and CSTB have significantly higher fraction of cells with TKS5+ invadopodia (Figure 5H, Figure S5E).

Invadopodia utilize MMPs to degrade the ECM; in fact, invasive cancer cells secrete proteases such as MMPs and cathepsins to promote invasion (22,23). We therefore tested the protease activity in cells that overexpress the three proteins, using fluorescein-conjugated peptides that are quenched and can be activated by protease cleavage (Figure 5I) (20). The substrates tested were largely cleaved by recombinant MMPs (Q3, Q6, PQ19) or serine protease uPA (PQ2), but not by ADAMs or cathepsins (Figure 5J). We found that lysates from CSTB and SERPINB5 cells appear to express higher MMP but not uPA activity because they cleaved Q3, Q6 and PQ19 significantly better than did control cells, whereas AGRN did not affect the cleavage of the tested substrates (Figure 5K). Supporting these assignments of substrate specificity, EDTA significantly reduced the cleavage of Q3, Q6, and PQ19 but not of PQ2. Thus, these results suggest that SERPINB5 and CSTB likely promote extravasation through promoting invadopodia formation and MMP activity.

### **SERPINB5 protein levels released to desmoplastic stroma correlate with poor patient survival**

Kaplan-Meier survival analysis using TCGA RNAseq data showed that high mRNA expression levels of AGRN, SERPINB5, and CSTB correlate with poor survival (Figure 1E–G). We sought to investigate survival correlations at the protein level using IHC to examine SERPINB5 protein expression on a human PDAC tumor microarray comprising samples from 75 patients. We observed SERPINB5 staining both within the epithelial cells and associated with desmoplastic stroma (Figures 6 and S6A–C). We found that high SERPINB5 protein levels, when associated with the stroma, but not when associated with the epithelial cells, correlated with significantly poor patient survival (Figures 6A, B and S6A–C). To confirm the cellular origin of the stromally located SERPINB5 protein, we performed RNA *in situ* hybridization of SERPINB5 on clinical samples showing high stromal SERPINB5 score. We showed that SERPINB5 mRNA is exclusively present in the epithelial compartment (KRT19-positive) and is absent from cells in the desmoplastic region (Figure 6C), whereas the adjacent section showed high SERPINB5 protein levels associated with the extracellular matrix (Figure 6D). Therefore, the stromal SERPINB5 protein is produced by

the cancer cells and deposited into the extracellular stroma in some regions of PDAC tumors but not others. Supporting this secretion hypothesis, we identified SERPINB5 protein in the conditioned media from SERPINB5 overexpression BxPC3 cells (Figure S6D). Our SERPINB5 human TMA results are consistent with our previous xenograft MS data that SERPINB5 protein is exclusively made by cancer cells and conform with our *in vivo* finding that SERPINB5 appears to be a metastasis promoter in PDAC.

## DISCUSSION

### Cancer-cell-derived matrisome proteins promote cancer progression

PDAC is known for its abundant ECM. Methods to deplete the bulk matrix in PDAC have not led to successful outcomes. Tumor microenvironment includes many types of cells, including different fibroblasts, immune cells, endothelial cells, fat cells, and neuronal cells, all of which could deposit matrisome proteins. It has long been known that fibroblasts deposit ECM proteins; however, it has only recently become evident that cancer cells also express many matrisome proteins during cancer progression and in various stress conditions and can play important roles in enhancing tumor progression (24). In our prior study, we identified a large number of cancer-cell-derived matrisome proteins elevated during PDAC progression, and showed that high expression of these tumor-cell-derived proteins correlates with poor patient survival (13). In this study we investigated whether these matrisome proteins play causal roles in PDAC tumorigenesis. We selected three cancer-cell-derived matrisome proteins, AGRN, SERPINB5 and CSTB, that are overrepresented in the PDAC ECM and performed *in vivo* functional analyses. We demonstrated that all three could promote metastasis at different steps of the metastatic cascade based on consistent results from both overexpression and knockdown experiments.

The overexpression experiments used the BxPC3 cell line that is KRAS wild-type and SMAD4 mutant whereas the knockdown experiments were done in the AsPC1 cell line that is KRAS mutant and SMAD4 wild-type. Thus AGRN, SERPINB5, and CSTB apparently promote metastasis independent of which signaling pathways (KRAS or SMAD4/TGFbeta) initiate metastasis. These three proteins likely represent downstream players common to both initiating stimuli.

In order to understand how cancer cells extravasate from vasculature, for some assays (e.g., extravasation) we used a tail-vein-injection model, which primarily assesses metastasis to the lungs. However, lung is a less preferred metastatic site in PDAC patients as compared to the liver. Patients with first site of lung recurrence had a more favorable outcome compared to patients who recurred with liver metastasis as the first site of recurrence (25). Therefore, it is possible that cells metastasizing to the lung and liver use somewhat different mechanisms. The results of our orthotopic metastasis assays suggest that the three genes we have studied promote metastasis to both the lungs and the liver from the orthotopic site, however, the mechanisms of the latter metastatic cascade will need to be directly studied in the liver.

There are other examples of cancer-cell-derived matrisome proteins playing a role in tumorigenesis. Drug-resistant breast cancer cells significantly upregulate ECM components, which are hypothesized to provide protection to cancer cells (26). Circulating-tumor-cells



(CTCs) in PDAC exhibit a very high expression of ECM proteins (27). The functional consequences of some of the cancer-cell-expressed matrisome proteins have been implicated in cancers. For example, cancer cell-derived glycoprotein tenascin-C (TNC) initiates seeding of metastases before stroma-derived TNC takes over in breast cancer (10), and is further demonstrated to play positive roles in tumorigenesis and metastasis in multiple types of cancer, including melanoma and lung cancer (28,29). High SPARC expression in PDAC CTCs promotes cancer cell migration and invasiveness (27). Studies from our lab identified cancer-cell- vs. stromal-cell-derived-matrisome proteins by mass spectrometry in breast cancer, colon cancer, melanoma, and PDAC (7,8,30). We see repeated overrepresentation of certain cancer-cell-derived proteins across different cancer types, such as Laminin-332, some annexins, and some S100 proteins. Many of them have not been studied before and may play instrumental roles in cancer progression as the three genes (AGRN, SERPINB5 and CSTB) that we studied here.

Together the results from this study and our previous study as discussed above suggest that increased levels of tumor-cell-derived matrisome proteins could function to drive more aggressive tumor cell behaviors. Therefore, instead of the bulk matrix, cancer-cell-derived matrisome proteins, or their regulators, may be more valuable targets for therapeutic interventions.

### **AGRN is a promoter of metastasis in PDAC**

The heparin sulfate proteoglycan agrin is a basement-membrane component, best known for organizing postsynaptic differentiation at the neuromuscular junction. Recently, AGRN has been reported to be upregulated in hepatocellular carcinoma (HCC), as well as other types of cancer (31,32). In HCC, AGRN has been shown to be secreted from human hepatic stellate cells upon activation by platelet-derived growth factor (PDGF) and to relay mechanosensitive signals into cells to regulate focal adhesion kinase and promote EMT, proliferation, migration and invasion (31–33).

We report here that AGRN is overrepresented in the ECM of human and murine PDAC samples. Using our previously published MS dataset that allows assignment of cellular origin (epithelial tumor cell or microenvironmental stromal cell), we found that AGRN is produced predominantly by the tumor cells (about 25-fold more than stromal-cell-derived AGRN) (13). AGRN knockdown in the tumor cells reduced primary tumor growth moderately but significantly. However, overexpressing AGRN had no effect on primary tumor growth. In both knockdown and overexpression scenarios, AGRN levels were consistently correlated with metastatic potential. AGRN potentially promotes metastasis at multiple steps in the metastatic cascade. First, AGRN likely promotes metastasis through stimulation of the EMT program in the primary tumor, which could lead to increased migration, invasion, and dissemination of cancer cells from primary tumor sites. Consistent with our study, AGRN in cultured HCC cells has been shown to form a complex with Lrp4 and Musk, and this complex activates the FAK pathway which drives the EMT program (32). In other systems, FAK has been shown to promote EMT by transcriptional regulation of several mesenchymal markers and delocalization of E-cadherin (34). Second, because AGRN promotes pulmonary metastasis after tail-vein injection, yet with no impact on the



extravasation rate, AGRN could promote some later steps in the metastasis, such as colonization and outgrowth, which may also involve the EMT program. In support of this hypothesis, we found that AGRN promoted cancer cell ZEB-1 expression *in vivo* and it has been shown that ZEB-1 knockout PDAC cells from Pdx1-cre; Kras<sup>LSL.G12D/+</sup>; Tp53<sup>LSL.R172H/+</sup>; Zeb1<sup>fl/fl</sup> (KPCZ) mouse have reduced capacity for lung colonization, stemness and experimental metastasis capacity (35). Therefore, AGRN promotes metastasis potentially through driving EMT and enhancing other steps in the metastatic cascade.

### SERPINB5 is a promoter of metastasis in PDAC

SERPINB5, also known as Maspin, is a non-inhibitory member of the serine protease inhibitor superfamily. There are conflicting reports as to whether SERPINB5 promotes or suppresses cancer. First, SERPINB5 expression can increase or decrease in cancers in a context-dependent fashion. It is downregulated in several types of cancers, including breast and prostate cancer and melanoma, and upregulated in several other types of cancers, including PDAC, gallbladder, thyroid, and colorectal cancers (36,37). Second, there are conflicting data regarding correlation of SERPINB5 expression with clinical outcomes and prognostic implications in multiple types of cancers, such as breast cancer, thyroid, gastric and colorectal cancers (37). SERPINB5 was traditionally identified as a tumor suppressor and was shown to inhibit cancer cell migration, invasion, and to induce apoptosis largely in breast cancer models (37). However, the *in vivo* function of SERPINB5 has not been studied in cancer contexts where SERPINB5 is upregulated.

In PDAC, SERPINB5 expression is observed in PanINs and PDAC but not in normal pancreas (38,39), meanwhile SERPINB5 overexpression correlates with worse prognosis in PDAC patients (38,40). Here we first confirmed that SERPINB5 is overrepresented at both RNA and protein level in human and mouse PDAC. We then demonstrated using both overexpression and knockdown systems that SERPINB5 promotes both spontaneous and experimental PDAC metastases, at least partially through enhancing invadopodia formation, tumor-cell extravasation and potentially MMP activity. Concordant with our data, SERPINB5 mRNA level positively correlated with metastasis potential in a panel of PDAC cell lines (41). *In vitro*, SERPINB5 overexpression led to more invasive PDAC cancer cells (42). Therefore, in PDAC, SERPINB5 functions as a metastasis promoter.

SERPINB5 was suggested to be secreted and deposited in the ECM in normal mammary epithelial cells (37,43). However, survival correlation studies were carried out only on intracellular SERPINB5 in cancers (13). How extracellular SERPINB5 may correlate with patient outcome has not been studied. Here, we demonstrated that high SERPINB5 staining of the desmoplastic stroma is a poor prognostic indicator in PDAC human patients. We further showed that SERPINB5 mRNA is exclusively made by the epithelial cells. Consistently, our previous MS analysis discovered SERPINB5 as exclusively produced by cancer cells and it is the second most abundant PDAC cancer-cell-derived SERPIN out of ten total SERPINs identified in the enriched ECM of xenograft tumors (13). SERPINB5 protein may arrive at the non-epithelial compartment through a variety of routes, such as secretion or being passively released from dying cancer cells. Supporting the secretion hypothesis, SERPINB5 protein is detected in the conditioned media of BxPC3 PDAC cells

overexpressing SERPINB5. More studies need to be carried out to understand the functions of SERPINB5 in the (extra)cellular-compartment and the correlation between SERPINB5 localization and survival in PDAC and other types of cancers.

### **CSTB also promotes metastasis in PDAC**

CSTB (cystatin B) is a cysteine protease inhibitor of the cystatin superfamily. Dysregulated expression of CSTB has been implicated in various cancers such as HCC and ovarian clear cell carcinoma (44,45). CSTB seems to play different roles in different types of cancer. CSTB deficiency reduces primary tumor growth via sensitization of tumor cells to oxidative stress in the PyMT murine mammary cancer model (46). In contrast, CSTB downregulation could promote cell proliferation and migration in a gastric cancer cell line (47). CSTB is known to be an inhibitor of cathepsin proteases, which are frequently upregulated in multiple types of cancer (48). Increased cathepsin expression generally correlates with increased malignancy and poor patient prognosis, however, individual cathepsins may have context-dependent tumor-suppressing roles (48). For example, CTSL serves as a negative prognostic marker while CSTB serves as a positive prognostic marker in head and neck cancer patients (49). CSTB also has cathepsin-independent functions. CSTB deficiency sensitizes thymocytes to staurosporine-induced apoptosis, and this function of CSTB is independent of cysteine cathepsins (50).

In our study, we found that CSTB promoted extravasation from the lung vasculature, leading to increased metastatic load in a tail-vein metastasis model. The increased extravasation rate may be due to the increased invadopodia formation observed upon CSTB overexpression. Consistent with the enhanced invadopodia formation, we observed increased cellular proteolytic activity that most likely belongs to the MMP family. Further investigation is required as to how CSTB promotes invadopodia formation and promotes metastasis, and whether such function requires inhibition of cathepsins, and if so, which cathepsins. Our previous TMT-MS data revealed some consistently overrepresented cathepsins in both human and mouse PDAC, including CTSB, CTSC, CTSD, CTSE, CTSG, CTSK, CTSL, and CTSS (13). They could be CSTB candidate targets and that should be further investigated.

We describe here functional *in vivo* characterization following up our previous comprehensive proteomic study of PDAC ECM, which suggested that, unlike stromal-cell-derived matrisome proteins, cancer cells selectively upregulate matrisome proteins that correlate with poor patient outcomes. In this study, we selected three proteins, whose functional implications in PDAC have not been previously studied *in vivo*. We provide *in vivo* data that all three are metastasis promoters and function in distinct steps of the metastatic cascade. These mechanistic studies of these three proteins not only provide novel insights into their biological roles in PDAC, but also support the notion that cancer-cell-derived matrisome proteins are pro-tumorigenic and are potentially better therapeutic targets that may not lead to the same adverse effects as does non-selectively depletion of the bulk matrix.

### **Supplementary Material**

Refer to Web version on PubMed Central for supplementary material.

## ACKNOWLEDGEMENTS

We thank the Hope Babette Tang Histology Facility at the Koch Institute Swanson Biotechnology Center for technical assistance; David Benjamin for help with ImageJ quantification; Roderick Bronson for pathological analysis and Anette Berglund for technical assistance.

C.T. was a Sherry and Alan Leventhal Family Fellow of the Damon Runyon Cancer Research Foundation. This work was supported by the STARR Cancer Consortium (to ROH and DAT), the Howard Hughes Medical Institute, of which ROH was an investigator, and the Lustgarten Foundation, where D.A.T. is a distinguished scholar and Director of the Lustgarten Foundation-designated Laboratory of Pancreatic Cancer Research. Support was also provided by NCI Cancer Center Support Grants to MIT, Koch Institute (P30CA14051-45) and Cold Spring Harbor (P30CA45508-27) and shared resources of the St. Giles Foundation Microscopy Center, Animal & tissue imaging, and the Animal Facility, both at CSHL. D.A.T. is also supported by the Cold Spring Harbor Laboratory Association, the NIH (5P30CA45508-27, 1U10CA180944-04, and 1R01CA190092-04, 5P20CA192996-03, 1U01CA210240-01A1), the DOD (W81XWH-13-PRCRP-IA), and the V Foundation. S.R. and C.T. were supported by postdoctoral fellowships from the MIT Ludwig Center for Molecular Oncology. D.Ö was supported by: the Swedish Research Council (537-2013-7277 and 2017-01531), the Kempe Foundations (JCK-1301) the Swedish Society of Medicine (SLS-326921, SLS-250831, SLS- 175991, and SLS-591551), federal funds through the county council of Västerbotten (ALFVLL369081, VLL-643451), the Cancer Research Foundation in Northern Sweden (AMP15-793 and AMP 17-877), the Swedish Foundation for International Cooperation in Research and Higher Education (PT2015-6432), the Knut and Alice Wallenberg foundation and the Swedish Cancer Society (CAN 2017/332 and CAN 2017/827). This study was also supported in part by a Koch Institute Support Grant No. P30-CA14051 from the National Cancer Institute (Swanson Biotechnology Center), and a Core Center Grant P30-ES002109 from the National Institute of Environmental Health Sciences, the Ludwig Fund for Cancer Research and the Koch Institute's Marble Center for Cancer Nanomedicine. S.N.B. is a Howard Hughes Medical Institute Investigator.

## REFERENCES

1. Siegel RL, Miller KD, Jemal A. Cancer statistics, 2019. *CA Cancer J Clin* 2019;69:7–34 [PubMed: 30620402]
2. Manji GA, Olive KP, Saenger YM, Oberstein P. Current and Emerging Therapies in Metastatic Pancreatic Cancer. *Clinical cancer research : an official journal of the American Association for Cancer Research* 2017;23:1670–8 [PubMed: 28373365]
3. Cid-Arregui A, Juarez V. Perspectives in the treatment of pancreatic adenocarcinoma. *World J Gastroenterol* 2015;21:9297–316 [PubMed: 26309356]
4. Rhim AD, Oberstein PE, Thomas DH, Mirek ET, Palermo CF, Sastra SA, et al. Stromal Elements Act to Restrain, Rather Than Support, Pancreatic Ductal Adenocarcinoma. *Cancer cell* 2014
5. Ozdemir BC, Pentcheva-Hoang T, Carstens JL, Zheng X, Wu CC, Simpson TR, et al. Depletion of carcinoma-associated fibroblasts and fibrosis induces immunosuppression and accelerates pancreas cancer with reduced survival. *Cancer cell* 2014;25:719–34 [PubMed: 24856586]
6. Amakye D, Jagani Z, Dorsch M. Unraveling the therapeutic potential of the Hedgehog pathway in cancer. *Nature medicine* 2013;19:1410–22
7. Naba A, Clauser KR, Lamar JM, Carr SA, Hynes RO. Extracellular matrix signatures of human mammary carcinoma identify novel metastasis promoters. *Elife* 2014;3:e01308 [PubMed: 24618895]
8. Naba A, Clauser KR, Hoersch S, Liu H, Carr SA, Hynes RO. The matrisome: in silico definition and in vivo characterization by proteomics of normal and tumor extracellular matrices. *Molecular & cellular proteomics : MCP* 2012;11:M111 014647
9. Pickup MW, Mouw JK, Weaver VM. The extracellular matrix modulates the hallmarks of cancer. *EMBO Rep* 2014;15:1243–53 [PubMed: 25381661]
10. Oskarsson T, Acharyya S, Zhang XHF, Vanharanta S, Tavazoie SF, Morris PG, et al. Breast cancer cells produce tenascin C as a metastatic niche component to colonize the lungs. *Nature medicine* 2011;17:867–U256
11. Malanchi I, Santamaria-Martinez A, Susanto E, Peng H, Lehr HA, Delaloye JF, et al. Interactions Between Breast Cancer Stem Cells and their Niche Govern Metastatic Colonization of the Lung. *Nature* 2012;48:S15–S

12. Socovich AM, Naba A. The cancer matrisome: From comprehensive characterization to biomarker discovery. *Seminars in cell & developmental biology* 2019;89:157–66 [PubMed: 29964200]
13. Tian C, Clauser KR, Ohlund D, Rickelt S, Huang Y, Gupta M, et al. Proteomic analyses of ECM during pancreatic ductal adenocarcinoma progression reveal different contributions by tumor and stromal cells. *Proceedings of the National Academy of Sciences of the United States of America* 2019;116:19609–18 [PubMed: 31484774]
14. Boj SF, Hwang CI, Baker LA, Chio II, Engle DD, Corbo V, et al. Organoid models of human and mouse ductal pancreatic cancer. *Cell* 2015;160:324–38 [PubMed: 25557080]
15. Konermann S, Brigham MD, Trevino AE, Joung J, Abudayyeh OO, Barcena C, et al. Genome-scale transcriptional activation by an engineered CRISPR-Cas9 complex. *Nature* 2015;517:583–8 [PubMed: 25494202]
16. Gilbert LA, Horlbeck MA, Adamson B, Villalta JE, Chen Y, Whitehead EH, et al. Genome-Scale CRISPR-Mediated Control of Gene Repression and Activation. *Cell* 2014;159:647–61 [PubMed: 25307932]
17. Sharma VP, Entenberg D, Condeelis J. High-resolution live-cell imaging and time-lapse microscopy of invadopodium dynamics and tracking analysis. *Methods Mol Biol* 2013;1046:343–57 [PubMed: 23868599]
18. Baik M, French B, Chen YC, Byers JT, Chen KT, French SW, et al. Identification of invadopodia by TKS5 staining in human cancer lines and patient tumor samples. *MethodsX* 2019;6:718–26 [PubMed: 31011543]
19. Bailey P, Chang DK, Nones K, Johns AL, Patch AM, Gingras MC, et al. Genomic analyses identify molecular subtypes of pancreatic cancer. *Nature* 2016;531:47–52 [PubMed: 26909576]
20. Dudani JS, Ibrahim M, Kirkpatrick J, Warren AD, Bhatia SN. Classification of prostate cancer using a protease activity nanosensor library. *Proceedings of the National Academy of Sciences of the United States of America* 2018;115:8954–9 [PubMed: 30126988]
21. Brabletz T, Kalluri R, Nieto MA, Weinberg RA. EMT in cancer. *Nature reviews Cancer* 2018;18:128–34
22. Leong HS, Robertson AE, Stoletov K, Leith SJ, Chin CA, Chien AE, et al. Invadopodia are required for cancer cell extravasation and are a therapeutic target for metastasis. *Cell reports* 2014;8:1558–70 [PubMed: 25176655]
23. Weaver AM. Invadopodia: specialized cell structures for cancer invasion. *Clin Exp Metastasis* 2006;23:97–105 [PubMed: 16830222]
24. Gao-Feng Xiong RX. Function of cancer cell-derived extracellular matrix in tumor progression. *J Cancer Metastasis Treat* 2016;2016;2:357–64.
25. Sahin IH, Elias H, Chou JF, Capanu M, O'Reilly EM. Pancreatic adenocarcinoma: insights into patterns of recurrence and disease behavior. *BMC Cancer* 2018;18:769 [PubMed: 30055578]
26. Iseri OD, Kars MD, Arpacı F, Gunduz U. Gene expression analysis of drug-resistant MCF-7 cells: implications for relation to extracellular matrix proteins. *Cancer Chemother Pharmacol* 2010;65:447–55 [PubMed: 19543729]
27. Ting DT, Wittner BS, Ligorio M, Vincent Jordan N, Shah AM, Miyamoto DT, et al. Single-cell RNA sequencing identifies extracellular matrix gene expression by pancreatic circulating tumor cells. *Cell reports* 2014;8:1905–18 [PubMed: 25242334]
28. Gocheva V, Naba A, Bhutkar A, Guardia T, Miller KM, Li CM, et al. Quantitative proteomics identify Tenascin-C as a promoter of lung cancer progression and contributor to a signature prognostic of patient survival. *Proceedings of the National Academy of Sciences of the United States of America* 2017;114:E5625–E34 [PubMed: 28652369]
29. Lowy CM, Oskarsson T. Tenascin C in metastasis: A view from the invasive front. *Cell Adh Migr* 2015;9:112–24 [PubMed: 25738825]
30. Naba A, Clauser KR, Whittaker CA, Carr SA, Tanabe KK, Hynes RO. Extracellular matrix signatures of human primary metastatic colon cancers and their metastases to liver. *BMC Cancer* 2014;14:518 [PubMed: 25037231]
31. Chakraborty S, Njah K, Pobbati AV, Lim YB, Raju A, Lakshmanan M, et al. Agrin as a Mechanotransduction Signal Regulating YAP through the Hippo Pathway. *Cell reports* 2017;18:2464–79 [PubMed: 28273460]

32. Chakraborty S, Lakshmanan M, Swa HL, Chen J, Zhang X, Ong YS, et al. An oncogenic role of Agrin in regulating focal adhesion integrity in hepatocellular carcinoma. *Nature communications* 2015;6:6184
33. Lv X, Fang C, Yin R, Qiao B, Shang R, Wang J, et al. Agrin para-secreted by PDGF-activated human hepatic stellate cells promotes hepatocarcinogenesis in vitro and in vivo. *Oncotarget* 2017;8:105340–55 [PubMed: 29285255]
34. Yoon H, Dehart JP, Murphy JM, Lim ST. Understanding the roles of FAK in cancer: inhibitors, genetic models, and new insights. *J Histochem Cytochem* 2015;63:114–28 [PubMed: 25380750]
35. Krebs AM, Mitschke J, Laserra Losada M, Schmalhofer O, Boerries M, Busch H, et al. The EMT-activator Zeb1 is a key factor for cell plasticity and promotes metastasis in pancreatic cancer. *Nature cell biology* 2017;19:518–29 [PubMed: 28414315]
36. Berardi R, Morgese F, Onofri A, Mazzanti P, Pistelli M, Ballatore Z, et al. Role of maspin in cancer. *Clin Transl Med* 2013;2:8 [PubMed: 23497644]
37. Bodenshteyn TM, Seftor RE, Khalkhali-Ellis Z, Seftor EA, Pemberton PA, Hendrix MJ. Maspin: molecular mechanisms and therapeutic implications. *Cancer Metastasis Rev* 2012;31:529–51 [PubMed: 22752408]
38. Cao D, Zhang Q, Wu LS, Salaria SN, Winter JW, Hruban RH, et al. Prognostic significance of maspin in pancreatic ductal adenocarcinoma: tissue microarray analysis of 223 surgically resected cases. *Mod Pathol* 2007;20:570–8 [PubMed: 17396143]
39. Maass N, Hojo T, Ueding M, Luttes J, Kloppel G, Jonat W, et al. Expression of the tumor suppressor gene Maspin in human pancreatic cancers. *Clinical cancer research : an official journal of the American Association for Cancer Research* 2001;7:812–7 [PubMed: 11309327]
40. Lim YJ, Lee JK, Jang WY, Song SY, Lee KT, Paik SW, et al. Prognostic significance of maspin in pancreatic ductal adenocarcinoma. *Korean J Intern Med* 2004;19:15–8 [PubMed: 15053038]
41. Mardin WA, Petrov KO, Enns A, Senninger N, Haier J, Mees ST. SERPINB5 and AKAP12 - expression and promoter methylation of metastasis suppressor genes in pancreatic ductal adenocarcinoma. *BMC Cancer* 2010;10:549 [PubMed: 20939879]
42. Hong SN, Lee JK, Choe WH, Ha HY, Park K, Sung IK, et al. The effect of aberrant maspin expression on the invasive ability of pancreatic ductal adenocarcinoma cells. *Oncol Rep* 2009;21:425–30 [PubMed: 19148518]
43. Khalkhali-Ellis Z, Hendrix MJ. Elucidating the function of secreted maspin: inhibiting cathepsin D-mediated matrix degradation. *Cancer research* 2007;67:3535–9 [PubMed: 17440060]
44. Takaya A, Peng WX, Ishino K, Kudo M, Yamamoto T, Wada R, et al. Cystatin B as a potential diagnostic biomarker in ovarian clear cell carcinoma. *Int J Oncol* 2015;46:1573–81 [PubMed: 25633807]
45. Lin YY, Chen ZW, Lin ZP, Lin LB, Yang XM, Xu LY, et al. Tissue Levels of Stefin A and Stefin B in Hepatocellular Carcinoma. *Anat Rec (Hoboken)* 2016;299:428–38 [PubMed: 26753874]
46. Butinar M, Prebanda MT, Rajkovic J, Jeric B, Stoka V, Peters C, et al. Stefin B deficiency reduces tumor growth via sensitization of tumor cells to oxidative stress in a breast cancer model. *Oncogene* 2014;33:3392–400 [PubMed: 23955077]
47. Zhang J, Shi Z, Huang J, Zou X. CSTB Downregulation Promotes Cell Proliferation and Migration and Suppresses Apoptosis in Gastric Cancer SGC-7901 Cell Line. *Oncol Res* 2016;24:487–94 [PubMed: 28281969]
48. Olson OC, Joyce JA. Cysteine cathepsin proteases: regulators of cancer progression and therapeutic response. *Nature reviews Cancer* 2015;15:712–29 [PubMed: 26597527]
49. Budihna M, Stojan P, Smid L, Skrk J, Vrhovec I, Zuperc A, et al. Prognostic value of cathepsins B, H, L, D and their endogenous inhibitors stefins A and B in head and neck carcinoma. *Biol Chem Hoppe Seyler* 1996;377:385–90 [PubMed: 8839984]
50. Kopitar-Jerala N, Schweiger A, Myers RM, Turk V, Turk B. Sensitization of stefin B-deficient thymocytes towards staurosporin-induced apoptosis is independent of cysteine cathepsins. *FEBS letters* 2005;579:2149–55 [PubMed: 15811333]

**Statement of Significance**

This study provides insights into the biological roles of cancer-cell-derived matrisome proteins in PDAC, and supports the notion that these proteins are pro-tumorigenic and better therapeutic targets.

Author Manuscript

Author Manuscript

Author Manuscript

Author Manuscript



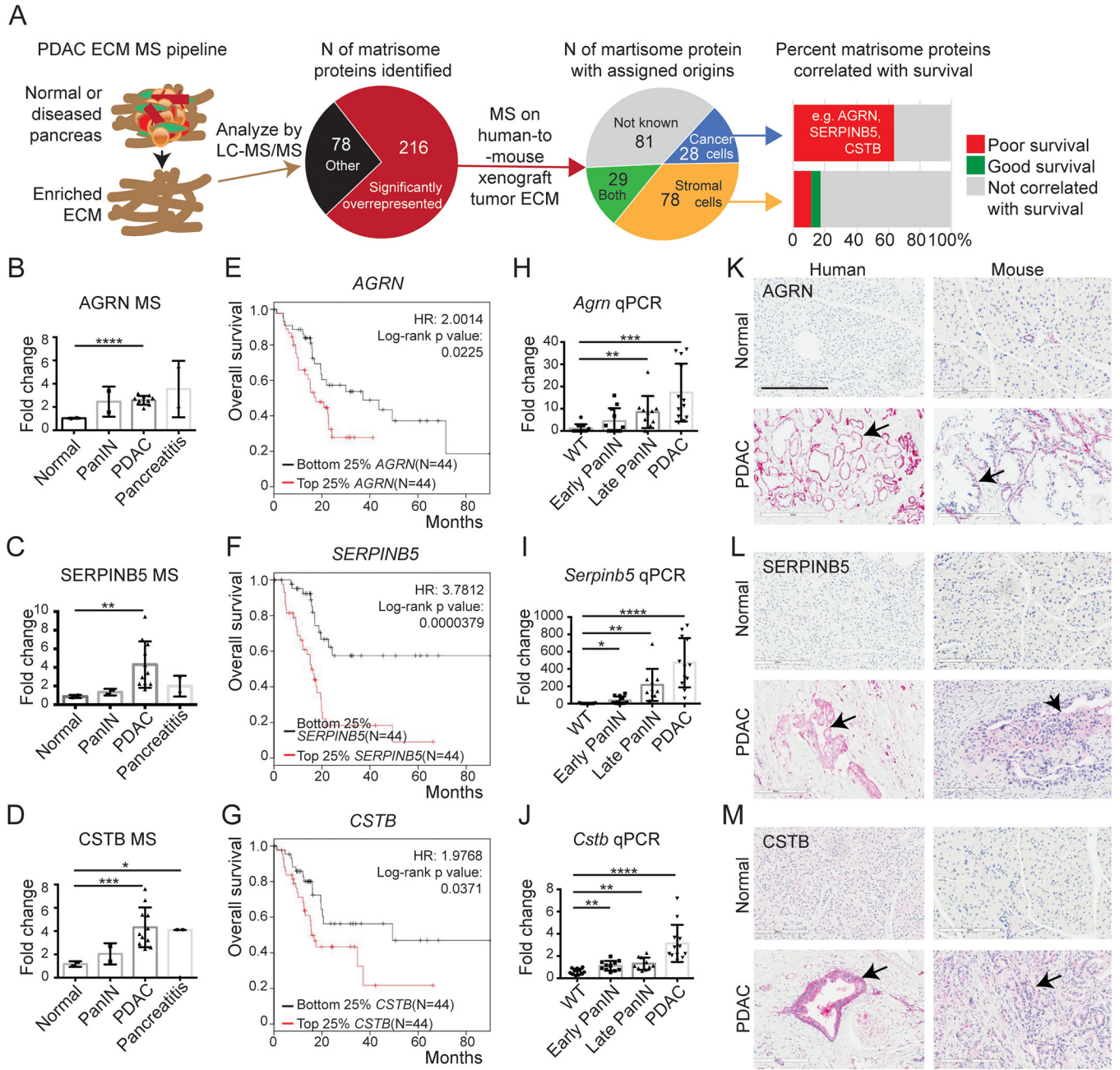


**Figure 1. Expression of AGRN, SERPINB5 and CSTB in PDAC and correlation with patient survival.**

A, a proteomic pipeline was used to identify overrepresented matrisome proteins in PDAC, and these proteins were then assigned as originating from human (cancer cell) or mouse (stroma) by MS analyses of human-to-mouse xenograft tumor ECM (13). Analyses of correlations with patient survival of individual matrisome proteins of different origins identified cancer-cell-derived matrisome proteins as being correlated with poor patient overall survival (e.g. AGRN, SERPINB5, and CSTB) whereas stromal-cell-derived proteins correlated either with good or poor survival and many showed no correlation with survival.



B-D, quantitative TMT MS/MS reporter-ion ratios normalized to normal pancreas in human samples show increasing amounts of *AGRN* (B), *SERPINB5* (C), and *CSTB* (D) proteins during PDAC progression.

E-G, Kaplan-Meier analyses of TCGA RNA-seq data show that high expression levels of *AGRN* (E), *SERPINB5* (F), and *CSTB* (G) correlate with poor overall patient survival.

H-J, mRNA levels of all three genes, *AgRN* (H), *Serpinb5* (I), and *Cstb* (J), are significantly elevated during PDAC progression in KC/KPC mouse samples, as shown by qRT-PCR.

K-M, Immunohistochemistry confirmed protein overexpression in human and mouse PDAC compared to normal samples. Arrows point to epithelial regions. Scale bar is 200 $\mu$ m.

\*,  $p < 0.05$ ; \*\*,  $p < 0.01$ ; \*\*\*,  $p < 0.001$ ; \*\*\*\*,  $p < 0.0001$ . ns, not significant. All p-values come from two-tailed t-tests. All columns are represented by mean  $\pm$  SD. This labeling scheme applies to all related figures.

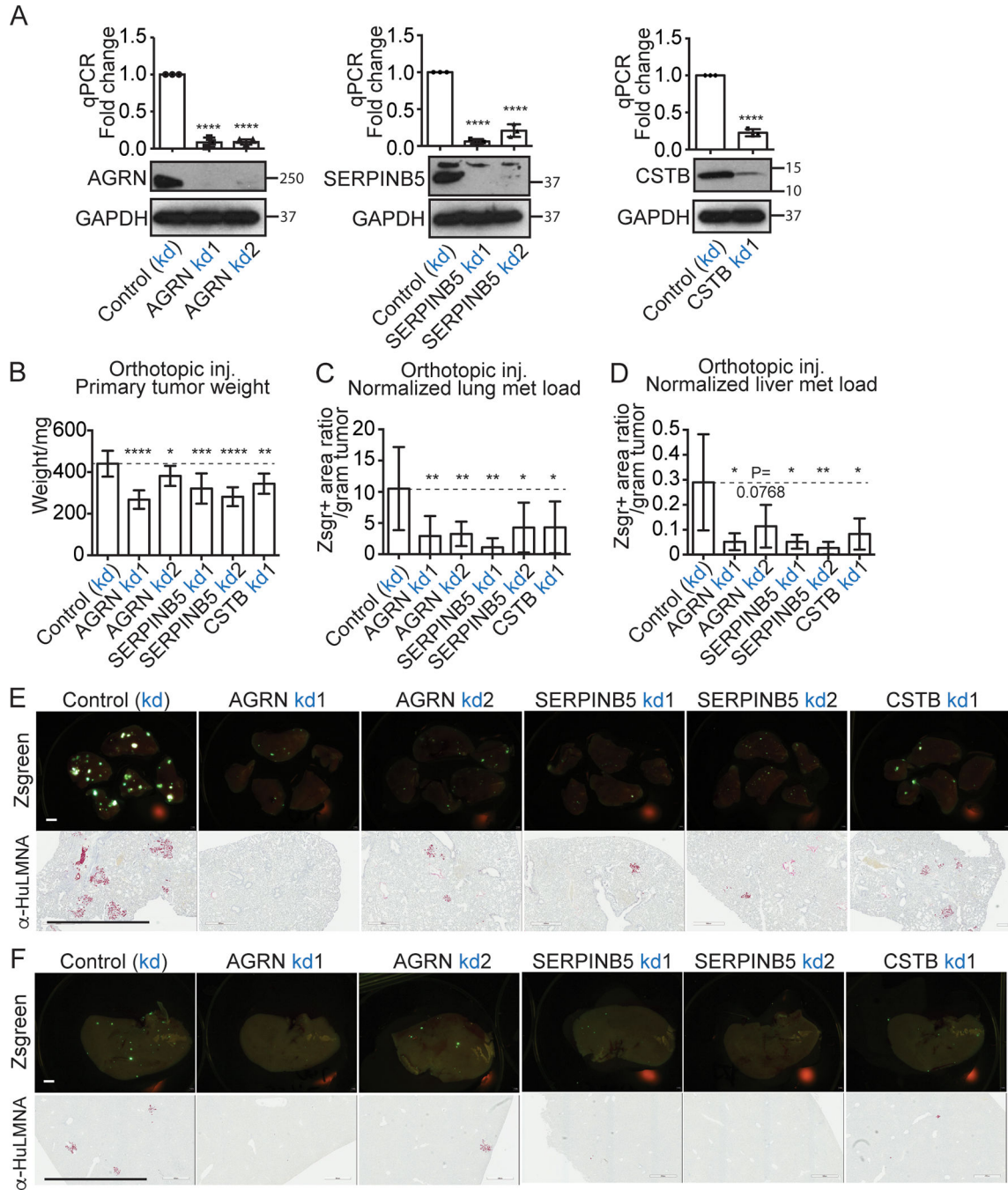


**Figure 2. Effects of knocking down expression of AGRN, SERPINB5, and CSTB on primary tumor growth and lung metastasis.**

A, CRISPR-inactivation (kd) knocked down expression in the BxPC3 G1.1 cell line, of AGRN, SERPINB5 and CSTB, respectively, as shown by qPCR (top) and western blot (WB) (bottom). GAPDH is the loading control.

B,C,D orthotopic injection of BxPC3 G1.1 cells knocked down for AGRN, SERPINB5, or CSTB showed that inhibition of each of them significantly reduced primary tumor weight (B), lung (C) and liver (D) metastasis load after normalization to primary tumor weight (C). N numbers are 12, 8, 9, 8, 10, 7 (left to right).

E,F, lung (E) and liver (F) metastasis images from CRISPR-inactivation orthotopic xenograft mice are shown.

Zsreen (upper rows) and human-specific LMNA staining (bottoms rows) both highlight cancer cells; scale bar is 2mm.

Author Manuscript

Author Manuscript

Author Manuscript

Author Manuscript

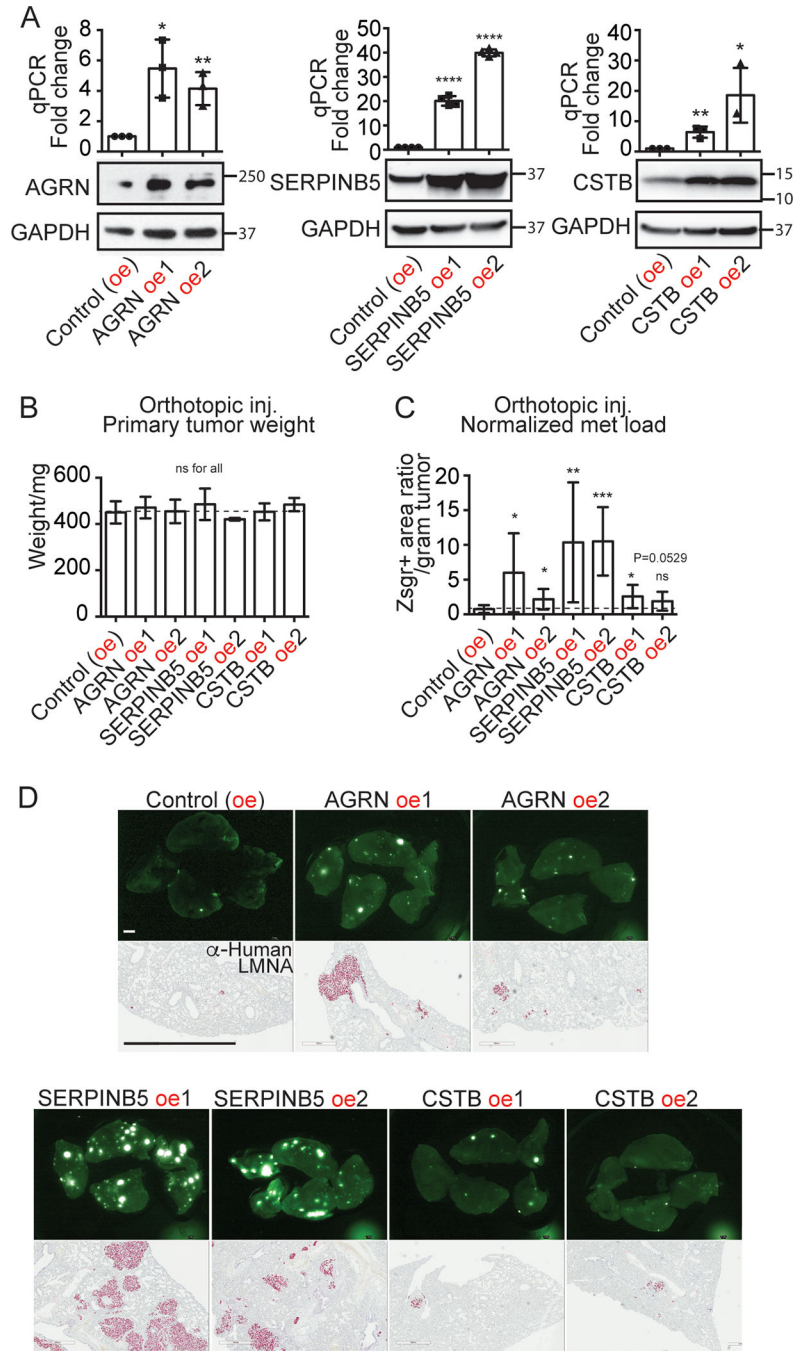


**Figure 3. Effects of overexpressing AGRN, SERPINB5, and CSTB on primary tumor growth and lung metastasis.**

A, CRISPR-SAM-induced overexpression (oe) in the AsPC1 cell line, overexpressed AGRN, SERPINB5 and CSTB, respectively, as shown by qPCR (top) and western blot (WB) (bottom). GAPDH is the loading control.

B, C, orthotopic injection of AsPC1 overexpressing AGRN, SERPINB5, or CSTB showed that overexpression of each of them failed to affect primary tumor weight (B). However, overexpression significantly increased lung metastasis load after normalization to primary tumor weight (C), except for CSTB oe2, for which P=0.0529.

N numbers are 8, 6, 7, 6, 5, 5, 6 (left to right).

D, lung images from CRISPR-SAM orthotopic xenograft mice are shown.

Zsreen (upper rows) and human-specific LMNA staining (bottom rows) both highlight cancer cells; scale bar is 2mm.

Author Manuscript

Author Manuscript

Author Manuscript

Author Manuscript



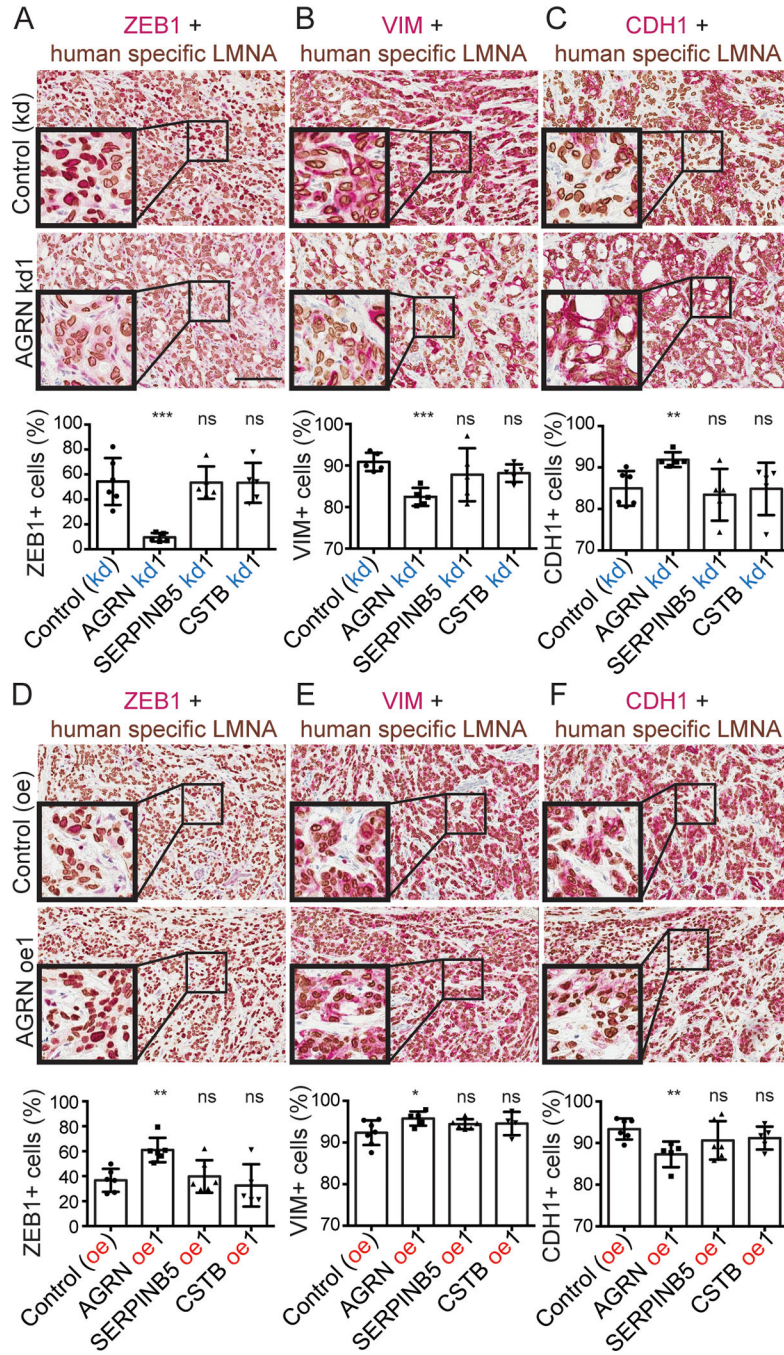


**Figure 4. AGRN promote EMT in primary tumors.**

A-F, double-color IHC with human-specific LMNA in brown and ZEB1 (A,D), VIM (B,E), or CDH1 (C,F) in red. The corresponding quantifications (see Materials and Methods) show that AGRN kd, but not SERPINB5 or CSTB kd, reduced ZEB1+ and VIM+ tumor-cell fractions and increased the CDH1+ tumor-cell fraction, while AGRN oe regulated EMT in the opposite direction.

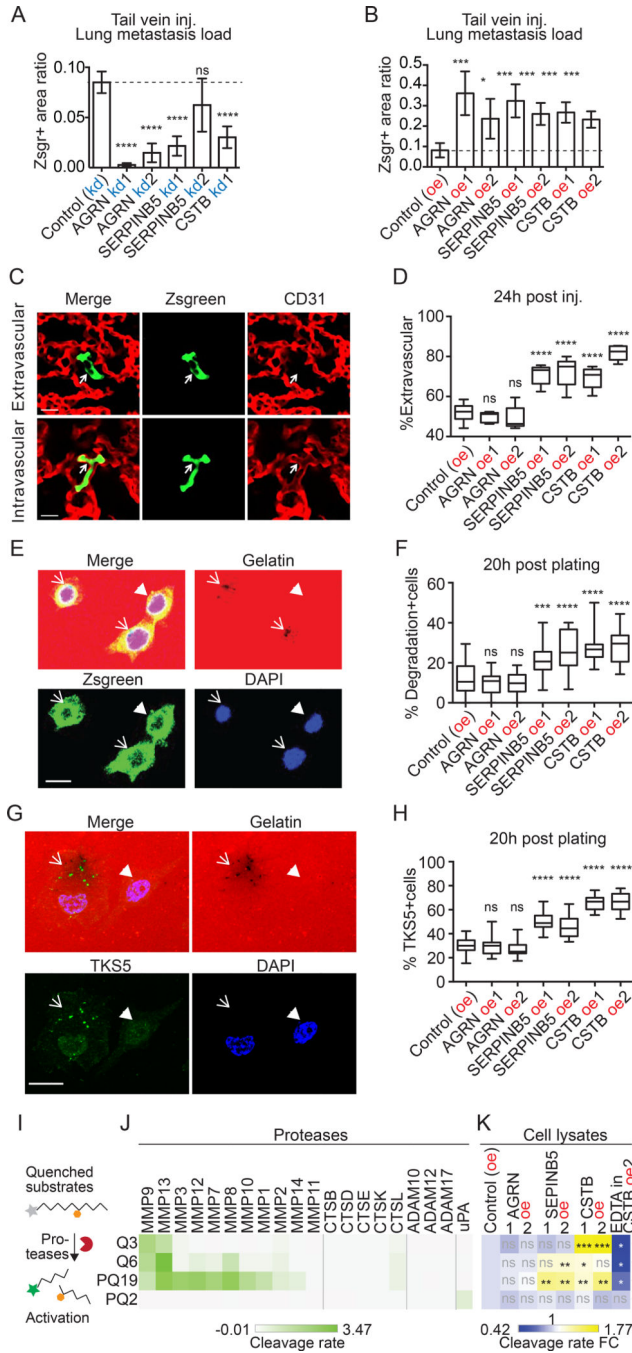


**Figure 5. SERPINB5 and CSTB promote formation of invadopodia and extravasation.**

A, B, tail-vein injection showed that knockdown (kd, A) of each of the three genes restricted, while overexpression (oe, B) of each promoted experimental metastasis. N=5 for all.

C, example images of cells that are inside or outside of vasculature 24h after tail-vein injection. Arrows point to cancer cells that are Zsgreen-positive.

D, extravasation assay shows that overexpression of either SERPINB5 or CSTB (but not AGRN) caused a higher fraction of cancer cells to be extravasated at 24h post-injection. At



least 40 cells were scored blindly per mouse. N=5 for all, except that N=10 for control group.

E, example images of cells that degraded (arrows) or did not degrade (arrowhead) gelatin in the course of invadopodial assays.

F, quantification of percentage of cells per field that have degraded gelatin at 20 hours post-plating for each cell line.

G, colocalization of TKS5+ invadopodia and the degradation spots in AsPC1 cells that degraded (arrow) or did not degrade (arrowhead) gelatin 20 hours post-plating.

H, quantification of percentage of cells per field that have TKS5+ invadopodia at 20 hours post-plating for each cell line. At least 20 fields were quantified per cell line for F and H (see Materials and Methods).

I, protease activity assay uses peptides with quenched fluorescein that can be dequenched by protease cleavage.

J,K, four peptides were cleaved by recombinant proteases (J) or cell lysates (K) in triplicate. Average cleavage rate is illustrated (J) and compared to the control cell lines (K).

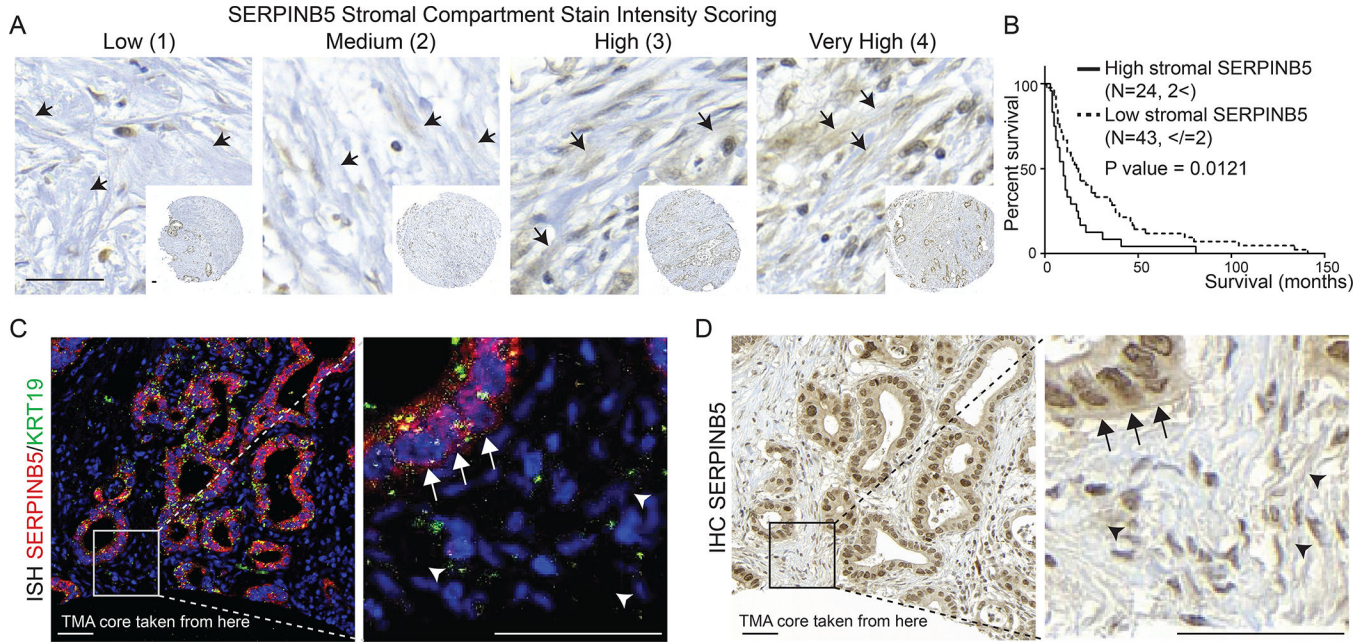


**Figure 6. Cancer-cell-derived SERPINB5 is a poor prognostic factor.**

A, representative images for stromal SERPINB5 staining scoring system on a human patient tissue microarray. Arrows point to representative stromal regions that look like ECM, where the scoring was done.

B, survival curves from patients categorized into two populations based on high and low stromal staining showed that high stromal signal correlates with significantly poorer patient survival.

C, D, RNA in situ hybridization showed exclusively epithelial-cell origin of SERPINB5 RNA (C), whereas the adjacent section (D), which was stained for SERPINB5 by IHC showed protein staining over the extracellular ECM (D). Arrows point to the epithelial compartment, while arrowheads point to the IHC signal over the ECM. Scale bars are 50µm.